ORIGINAL PAPER

Iron fouling prevention and membrane cleaning during reverse osmosis process

E. Melliti[1] · K. Touati[1] · H. Abidi[1] · H. Elfil[1]

Abstract

Fouling inhibition is one of the most important challenges in membrane processes. Manifesting under several forms and origins, fouling significantly reduces the performance of membranes during water desalination process. Despite its low concentration, iron is considered as one of the most common inorganic pollutants that generate oxides and hydroxides causing membrane fouling. In the current work, reverse osmosis (RO) membrane fouling caused by iron precipitation was investigated. Herein, the mechanism of iron salt crystallization by oxidation technique was experimentally studied. In addition, the regeneration of a fouled RO membrane by iron precipitation was carried out. Analysis with scanning electron microscopy, infrared (IR) and X-ray diffraction (DRX) spectroscopy has been performed to identify deposits. It was shown that the collected deposit is essentially the lepidocrocite (γ-FeOOH). RO membrane regeneration was carried out using citric acid as a cleaning reagent with a concentration of 0.01%. The efficiency of the treatment was tested through the assessment of the recovery ratio, pressure drop and iron accumulation. In addition, complexation–filtration using citric acid was tested to remove iron during pretreatment step to inhibit membrane fouling. IR and DRX data showed the complex iron citrate (Fe–citrate) was found in the RO retentate, which proves that the complexation–filtration process was clearly efficient.

Keywords Citric acid · Iron fouling · Membrane cleaning · Reverse osmosis

List of symbols

A	Water permeability coefficient (s/m)
C_0	Salt concentration (mg/L)
C_p	Permeate salt concentration (mg/L)
$C_{e,R}$	Retentate water concentration (mg/L)
D_e	Water diffusion coefficient (m²/s)
J_p	Water flux (m³/m² s)
ΔP_{long}	Longitudinal pressure drop (Pa)
ΔP	Applied pressure (Pa)
Q_F	Feed water flow (L/h)
Q_p	Permeate flow (L/h)
Q_R	Rejected water flow (L/h)
R_s	Salt rejection (%)
SHE	Standard hydrogen electrode (V)
T	Temperature (°C)
$V_{m,e}$	The molar volume of the water (m³/mol)

Greek letter

τ	Ions transformation rate (%)
τ_{acc}	Iron salt accumulation rate (%)
$\Delta\pi$	Osmotic pressure (Pa)
σ	Membrane boundary layer thickness (m)

✉ K. Touati
kha.touati@gmail.com

1 Laboratory of Natural Water Treatment, Water Researches and Technologies Center, B.P. 273, 8020 Soliman, Tunisia

Introduction

Water scarcity is one of the most important challenges nowadays. For that, several researches are carried out to find new alternatives sources of fresh water to overcome the high water demand. Desalination is now considered as a practical approach to secure drinking water supply for many countries around the world. Therefore, many researchers have focused on developing new technologies, so that desalination has been growing rapidly as a water production industry and as a field of research that combines engineering and science to develop innovative and economical means for water desalting. Nowadays, membrane processes are becoming one of

the most important versatile technologies. Reverse osmosis (RO) is one of the most worldwide used techniques to produce drinking water thanks to the quality of the water produced and the energy efficiency compared to other processes (Touati et al. 2017a; b). In this technique, organic and inorganic molecules are separated from a feed solution by solution diffusion mechanism (Peters 2010). Membranes are the key of the separation process. However, like any other membrane-based process, membranes are highly sensitive to organic, inorganic and biological fouling. Fouling is often correlated with the interactions between the membrane material and components of the activated sludge mixed liquor, which consists of solutes, colloidal and fine particles, microorganisms and other substances (Ji et al. 2016). These particles in feeding water deposit or entrap onto RO membrane surface, reduce the RO process efficiency (water recovery) and cause operational problems. Many researches are focusing on developing methods for prediction, prevention and mitigation of fouling. Several researches were based on the design of new membrane modules, the development of antifouling, and membranes cleaning. However, an efficient pretreatment process seems to be a fundamental way to mitigate this detrimental effect. The pretreatment consists of a series of unit operations that address each of the expected fouling risks for the purpose of keeping membranes in good condition and maintaining their performance reasonable period. Iron is often found in surface and ground waters worldwide at different concentration levels, usually up to 3–4 mg/L and in some cases up to 15 mg/L (Ellis et al. 2000). Iron presence can be linked to unusable esthetic, operational problems such as metallic taste of food, beverage and unpleasant odor (Al-Anber 2010). In water desalination using membrane, iron precipitation can drastically reduce the performance of the process. Several scientific researches have been realized to find new techniques for iron removal such as limestone filter treatment (Aziz et al. 2004), ash (Das et al. 2007), adsorption technique (Tahir and Rauf 2004) and oxidation using potassium and permanganate. Aeration, oxidation and separation are still the most used nowadays. However, none of these processes has found popularity due to their high costs and their complicated operation and maintenance requirements. Moreover, no attention has been paid to membrane regeneration in iron fouling. In the current work, understanding the mechanisms leading to the iron salt precipitation and finding an application as non-conventional pretreatment in a desalination pilot plant to prevent iron fouling were investigated. The idea is to trap iron by complexation and remove it in the rejected water without being fixed to the surface of the membrane. For that, a complexation reagent was chosen and tested. The choice of the reagent was based on several criteria such as low price, safety, simplicity of use and no damage to the process components. The efficiency of the inhibition was evaluated by the assessment of the RO membrane performance. For that, the recovery ratio of the process, the degree of chemical fouling of the membranes and its autopsy were studied.

Theoretical background

Membrane separation in RO

RO transport models can be classified into three main categories diffusion-based, pore and irreversible thermodynamic models (Hidalgo et al. 2011). When a system is constituted with a solvent and a neutral solute, Kedem and Katchalsky (1958) established phenomenological relationship of volume flow and the molar flow of solute in terms of three transport coefficients: the membrane reflection coefficient, its solute and water permeabilities. The transport of the solvent and solute through a perm-selective membrane is governed by the following equation:

$$J_P = A(\Delta P - \Delta \pi) \tag{1}$$

The water flux J_p of RO is proportional to the effective pressure ($\Delta P - \Delta \pi$). A is the water permeability coefficient, ΔP is the applied pressure, $\Delta \pi$ is the osmotic pressure difference on either side of the membrane. The salt rejection of the membrane R_s is defined as:

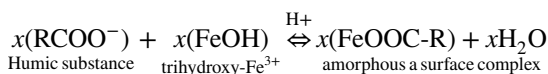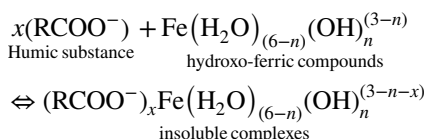$$R_s = \left(1 - \frac{C_p}{C_0}\right) \times 100 \tag{2}$$

where C_0 is the salt concentration of the inlet concentrated solution and C_p is the permeate concentration.

Iron chemistry

Iron complex formation with organic matter

The complexation of iron by organic matter is widely encountered in the nature. In fact, it occurs mainly in surface waters but also in some groundwater. Metals transported in anionic form in the water are reduced by humic, fulvic and tannic acids. This leads to a complex or a chelate of a cationic form of humic acids, which represent the major fraction

of natural organic matter (Tipping 1992). Humic substances play an essential role in the dissolution, transport and deposition of inorganic ions with a positive charge. Most of metals are able to form complexes with humic substances lying in the water. Complex formation can dramatically increase the solubility of the metal, e.g., humic substances naturally present in water make the iron up to a billion times more soluble (Shapiro 1964). There are also mixed complexes with common anions, particularly complex fulvic acid–iron phosphate (Owusu-Agyeman et al. 2007) and the complex fulvic acid–citrate, phosphate and copper salicylate (Manning and Ramamoorthy 1973). The reactions involved are likely to be numerous in view of the predominant presence of several ferric hydroxo-polymerized compounds (soluble and insoluble) and various organic material structures. One of the possible reactions is the formation of insoluble complexes between matters:

$$\underset{\text{Humic substance}}{x(RCOO^-)} + \underset{\text{hydroxo-ferric compounds}}{Fe(H_2O)_{(6-n)}(OH)_n^{(3-n)}}$$

$$\Leftrightarrow \underset{\text{insoluble complexes}}{(RCOO^-)_x Fe(H_2O)_{(6-n)}(OH)_n^{(3-n-x)}}$$

$$\underset{\text{Humic substance}}{x(RCOO^-)} + \underset{\text{trihydroxy-Fe}^{3+}}{x(FeOH)} \overset{H+}{\Leftrightarrow} \underset{\text{amorphous a surface complex}}{x(FeOOC\text{-}R)} + xH_2O$$

The iron oxides

Formed by iron atoms, oxygen and/or hydroxide of OH groups, the iron oxides are differentiated by their composition, the valence of iron ions and their crystallographic structure. To date, there are 16 kinds of iron oxy-hydroxides from crystallized compounds to amorphous compounds (Cornel and Schwertmann 1996). Among these oxides, one can mention: α-Fe_2O_3 (hematite), γ-Fe_2O_3 (maghemite), α-FeOOH (goethite), β-FeOOH (akaganeite) γ-FeOOH (lepidocrocite). The formation of these oxides and iron oxy-hydroxides depends on different parameters such as pH, oxygen content, relative humidity and also the electrolyte composition or contaminants. The equilibrium relations between the different iron oxides can be described by the E-pH equilibrium diagram (Fig. S1 supplementary content) developed by Descostes (2001) from the data Chivot (1998, 1999). According to this diagram, it is clear that the iron solubility increases with the acidity. Ferric iron is present when the solution electric potential E_H is more than 0.77 V/SHE; SHE is the standard hydrogen electrode. However, the range of stability of the ferrous ion is more extensive and these species are present in a E_H under 0.77 V/SHE.

Materials and methods

RO unit

The RO unit used in the current work is "Osmohom," manufactured by "Water Technology and Development" company. The capacity of this unit is around 10 L/h, and it is generally utilized for tap water with feed salinity lower than 2 g/L. The unit has five stages of filtration as indicated in Fig. 1. The
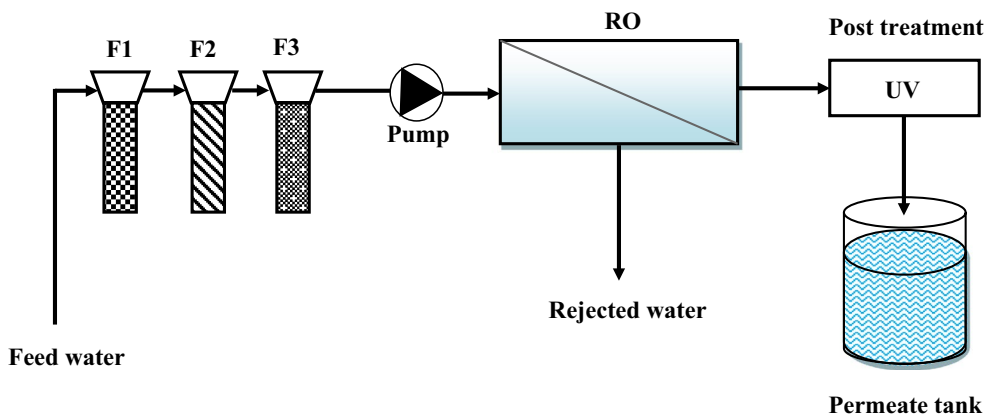

Fig. 1 Schematic of the RO unit. F1: cartridge filter. F2: granular activated carbon filter. F3: high-performance activated carbon filter. UV: post-treatment using ultraviolet radiations

pretreatment of the feed water consists of filtration through three cartridges. The first filter is a cartridge filter made of 100% polypropylene fibers. It removes rust particles and sediment with a diameter greater than 5 µm. The second cartridge is composed of granular activated carbon. Its particular construction ensures the percolation phenomenon: water passing axially through the carbon bed that creates a backwash avoiding any preferential path or bypass. The water remains in contact charcoal maximum time which ensures maximum adsorption. The third cartridge filter is composed of high-performance activated carbon. It removes organic contaminants, pesticides and especially chlorine that are very harmful to the RO membranes based on polyamide. The characteristics of the membrane (Model N^o TW30-1812-50) are provided by the manufacturer, and the membrane is constructed by polyamide. The recovery rate is around 20%, and the salt rejection is 90%. The physicochemical characteristics of the feed water are presented in Table 1.

Analytical techniques

X-ray diffraction

The diffractometer used was "Philips X'Pert PRO" brand that has a vertical goniometer (θ–2θ) configuration with direct optical coding for direct reading of the angular position of the goniometer arm and having a remarkable absolute angular precision of 0.0025° and a repeatability of less than 0.0001°. The diffractometer is operating at 45 kV and 40 mA, with a Cu X-ray tube ($\lambda = 0.15406$ nm) equipped with a 1×1 mm^2 point focus and a Nickel filter on the direct beam path to absorb the Cu K$_\beta$ radiation. The incident beam is collimated with a 1 mm. The deposit was recovered from precipitation tests by filtration on 0.45-µm membrane using

Büchner and dried in a desiccator for 4 h. The DRX sample was prepared in a powder sample holder (PW1811) as follows: Firstly, the sample holder ring was clamped securely to the preparation table. Then, the sample powder was pressed down firmly in the holder ring using the powder press block. The powder was spread in the holder ring, so that it is heaped up into a conical shape inside the holder ring. Finally, all surplus powder above the rim of the holder was removed using a knife blade.

Scanning electron microscope (SEM)

The SEM used in the current study is the QUANTA 200 Tare model (FEI Company). It was utilized to characterize the morphology of the deposit iron. The experiments with SEM were realized with an accelerating voltage of 15.0 kV.

Infrared spectroscopy (IR)

The IR spectra were collected using FTIR spectrometer IRAffinity-1 (Shimadzu, Japan). The spectral region was 4000–400 cm^{-1}, and the spectral resolution used was 2 cm^{-1}. The mean IR spectra were obtained using subsequent statistical processing. The preparation of powder sample for FTIR analysis was barely similar to DRX sample preparation. In this case, after being filtrated and dried, the recovered precipitate powder is incorporated in potassium bromide powder (KBr). A homogeneous mixture of about 1% sample/KBr powder was finely ground. The mixture was placed in a mold and then subjected to a very high pressure. It is then extracted from the mold in the form of a pellet. The sample holder containing the KBr/sample pellet was placed in the measuring compartment of the spectrometer on the path of the incident beam.

UV–visible

Iron is reduced with hydroxylamine chloride. It forms with ortho-phenanthroline a color of red–orange. The color intensity of the complex formed is measured by visible spectrophotometer (Shimadzu UV-1800) at a wave length of 510 nm.

Reagents

The ferrous chloride anhydrous reagent was with 98% purity and was purchased from Oxford Lab Chem. A citric acid with 99.8% purity, manufactured from R Company Hungary, was used. The citric acid solution concentration was 0.01%.

Table 1 Feed water characteristics

Ions	Concentration (mg/L)
Ca^{2+}	72.8
Mg^{2+}	64.15
HCO$_3^-$	373.93
Cl$^-$	337.25
Na$^+$	170.56
K$^+$	4.69
Conductivity (µs)	874
Salinity (mg/L)	556.94

Membrane fouling assessment

The study of the membrane fouling was carried out with a RO unit. The experiments were performed using a solution of $FeCl_2 \cdot 4H_2O$, with concentration range of 0.5 ppm of Fe^{2+}. Synthetic solution was stored in a 40-L tank and entered to the RO module using a feed pump.

Recovery ratio and pressure drop and iron retention rate over time measurement

Recovery ratio and pressure losses were used, as fundamental parameters, to assess the fouling. As shown in Fig. 2a, the recovery ratio declined gradually from 18% until 15.2%. This behavior is attributed to the decrease in the RO membrane performance. Crystal particles were accumulated on the membrane surface, which causes surface blockage and adds an additional resistance by building an extra layer. Therefore, the solvent diffusion becomes slower and the pressure drop
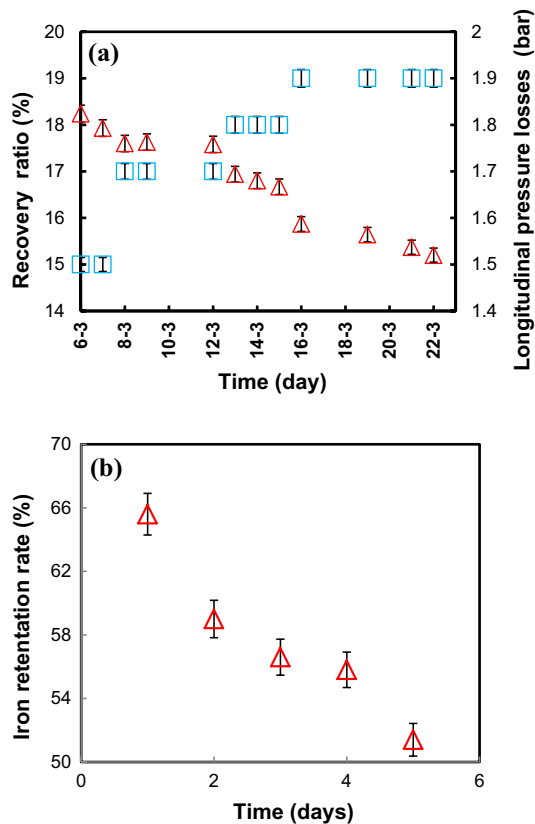
increases to reach 1.9 bars. As the iron is the only salt added in feed water and as mentioned previously, the deposit formed on the membrane surface is an iron oxy-hydroxide. This result correlates with many theoretical approaches. In fact, it was mentioned that iron fouling built on the membrane surface generates a progressive decline of the permeate flux, which can be considered the major factor influencing a long-term performance of the membrane. Consequently, the recovery ratio decreases as shown in previous results (Touati et al. 2017c, 2018a, b). Iron retention rate has been also assessed; in fact, Fig. 2b shows that the retention rate decreases gradually from 66% in the first day to 51.4% after 6 days of operation. This observation is attributed to the severe fouling that affected significantly the desalination process.

Iron salt accumulation rate during fouling

The variation of iron concentration was detected by UV spectroscopy. The accumulation factor was calculated as follows:

$$\tau_{acc} (\%) = 1 - \frac{Q_F \times \left[Fe^{2+}\right]_F}{Q_P \times \left[Fe^{2+}\right]_P + Q_R \times \left[Fe^{2+}\right]_R} \quad (3)$$

where τ_{acc} is the accumulation rate of the iron salt, $\left[Fe^{2+}\right]_P$, $\left[Fe^{2+}\right]_R$ and $\left[Fe^{2+}\right]_F$ were the iron concentrations (mol/L) in permeate, rejected and feed solutions, respectively. Q_F, Q_p and Q_R are the feed, permeate and rejected water flows, respectively. Since the iron precipitation has been depending on pH value, iron accumulation was examined as a function of time and pH. Figure 3 indicates that, for pH values less than 6, the accumulation rate of iron has no significant
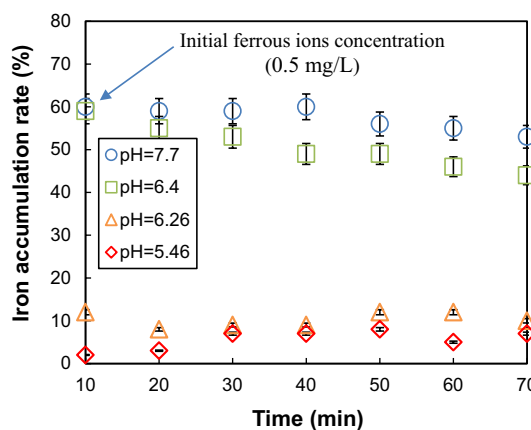

Fig. 2 a RO unit recovery ratio and pressure losses; b iron retention rate as function of time using iron solution ($[Fe^{2+}]_0 = 0.5$ ppm)

Fig. 3 Iron accumulation rate as a function of time during fouling tests. Initial ferrous solution concentration $[Fe^{2+}] = 0.5$ mg/L

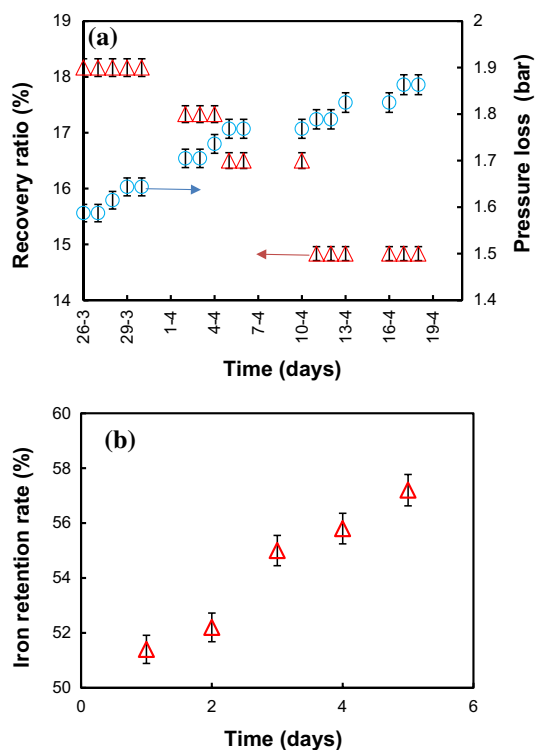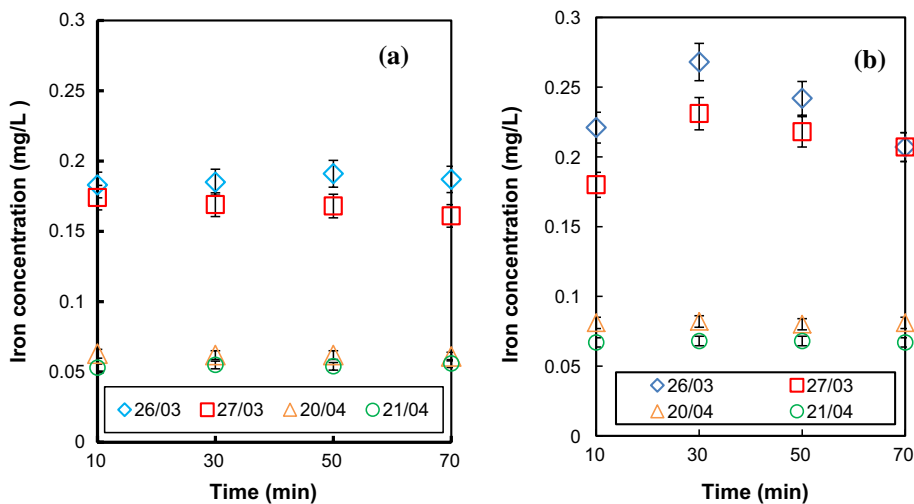**Fig. 4** **a** Recovery ratio and pressure losses; **b** iron retention rate as a function of time when using citric acid

solid leads to an increase in the membrane resistance and a severe reduction in the performance. Figure S2 (supplementary content) shows that the used RO membrane, compared to a new one, revealed a reddish color. This confirms the presence of iron precipitation on the RO membrane.

Results and discussion

Cleaning tests

Recovery ratio and pressure losses measurement

The cleaning test was carried out under backwashing process using a 0.01% of a citric acid solution. Figure 4 indicates that, for the second series of experiences, the recovery ratio starts to improve and tends to reach the performances of a virgin RO membrane (18%). Simultaneously, the pressure drop decreased from 1.9 bars to the value of 1.5 bars. Retention rate values (Fig. 4b) increased gradually to 58% after cleaning reagent addition. The results showed that the use of citric acid as a cleaning solution contributes to enhancing the RO performances. However, the action of citric acid on iron oxides is not well understood. In fact, there are two hypotheses that have been proposed to explain the mechanism: (1) Iron oxides were complexed by citric acid; (2) the citric acid is adsorbed on the iron oxides. These hypotheses will be studied in "Iron removal test" section.

Iron concentration measurement during the cleaning operation

Though iron presence promotes iron scale, a relationship between membrane cleaning efficiency and iron concentration can be established. Figure 5a, b shows a high iron

values. This experiment suggests that iron is still existing in the solution under ionic form. For pH < 6, the ferric iron oxidation has not yet occurred, while for a pH value between 6.4 and 7.7, an important increase in the iron accumulation rate was observed. It reached 60% at this pH range. It is clearly shown that the iron precipitation took place at pH value superior to 6. Sang and Morgan (1980) studied the kinetics of ferrous iron ions, and they found that for a pH value greater than 7 the ferrous iron disappears. This deposit

Fig. 5 Fe^{2+} concentrations in rejected water (**a**) and in the permeate (**b**) as a function of time during cleaning tests
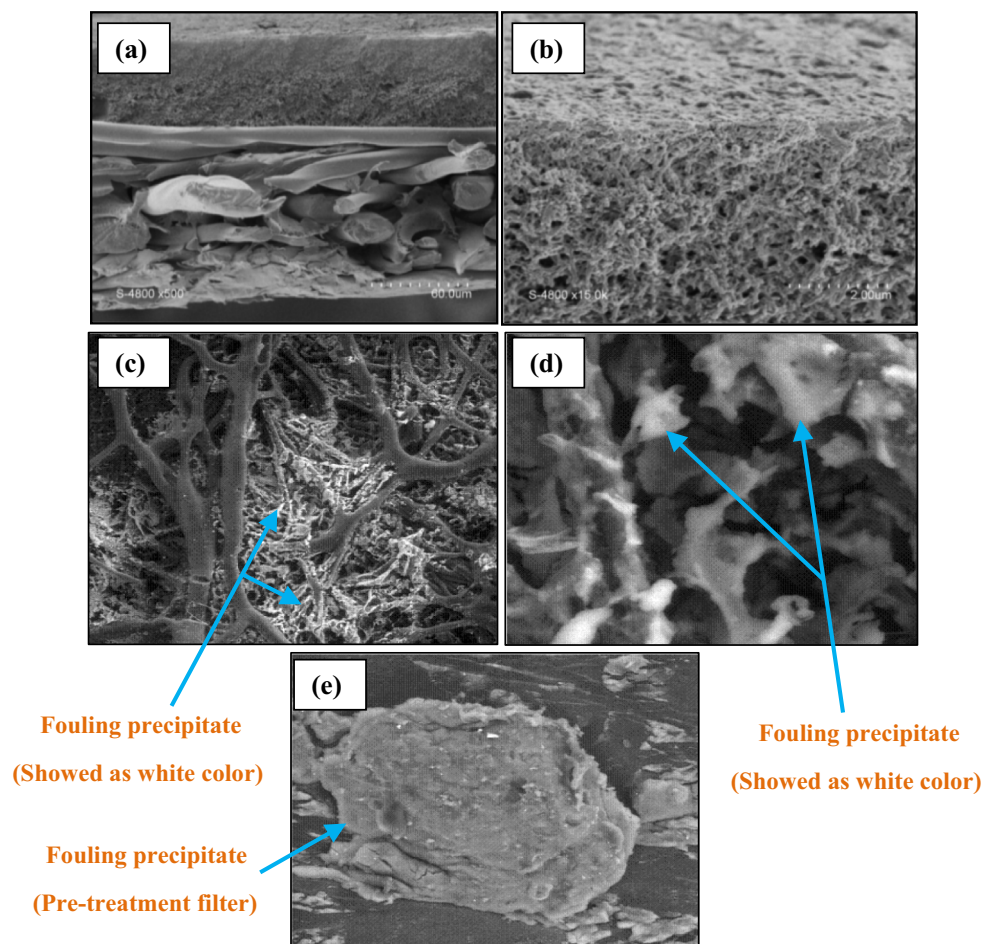
concentration in both permeate and rejected water, in the first days of cleaning process. However, after many hours of experimental running, the iron quantity decreased considerably and reached 0.05 and 0.07 mg/L in permeate and in rejected water, respectively. In fact, the addition of the citric acid as a cleaner reagent acts upon the iron oxides. The decrease in iron concentration accompanied with the increase in the membrane recovery (which means that the fouling layer was reduced or eliminated) affirms that the iron oxides have been reduced to iron ions. This hypothesis correlates with the observation of RO membrane after cleaning process (Fig. 4S supplementary content). The reddish scale disappears, and the RO membrane performance has been restored.

Membrane autopsy

The photograph (a) in Fig. 6 shows the asymmetric structure of a virgin RO membrane, in which a mechanical support coupled by a thin layer was detected. The photograph (b) shows the active layer of the RO membrane. Photographs (c) and (d) show fouled RO membrane with different magnifications. The scale formed on the cartridge filter in pretreatment step has been characterized and is presented in photograph (e). The iron crystals formed in these experiments showed a large variability in size, shape and thickness. Because of the strong dependence of crystal morphology on precipitation conditions such as oxygen content, humidity, and the characteristics of the surface that supports the precipitation, it is clear that iron precipitation conditions in RO membrane are different from those at the pretreatment filter. Then, the characteristics of the precipitate in the filter will be different from the one formed on the RO membrane surface. For that, to determinate the phase of the precipitate, the X-ray diffraction was used. Figure S3-a (supplementary content) represents the solids collected in pretreatment filter. In fact, it shows several bands that characterize the lepidocrocite γ-FeOOH. Figure S3-b (supplementary content) represents a diffractogram of a sample obtained from

Fig. 6 SEM images of **a** RO membrane structure ($\times$500); **b** membrane active layer structure ($\times$150), **c** fouled RO membrane ($\times$150), **d** fouled RO membrane ($\times$1300), **e** fouled filter membrane in pretreatment ($\times$600)

Fouling precipitate (Showed as white color)

Fouling precipitate (Pre-treatment filter)

Fouling precipitate (Showed as white color)

a fouled RO membrane. The bands of the diffractogram correspond to the goethite α-FeOOH. This observation suggests that γ-FeOOH, formed in the pretreatment filter, transforms to α-FeOOH. The latter one is thermodynamically more stable than the lepidocrocite form (Refait and Genin 1997).

Iron removal test

Iron–citric acid complexation

As previously demonstrated, citric acid can be used as a cleaning reagent to mitigate the iron fouling. In this section, the possibility of using the citric acid as an inhibitor of iron fouling was investigated. Citric acid, with the formula $H_3C_6H_5O_7$, is symbolized here as H_3Cit. Literature indicates that $FeCit^-$ and $FeOHCit^-$ are the species likely to precipitate in pH value of 7 (Hamm et al. 1954; Lanford and Quinan 1948; Bobtesky and Jordan 1947; Field et al. 1974). To confirm this hypothesis, XRD spectra measurements coupled by IR were used. Figure 7 illustrates the XDR spectra of the Cit^{3-} and of the Fe–Cit complex. Figure 7b shows that a new band, for the iron complex, appears at 600 cm^{-1}. The present of this band is due to the vibration of the Fe–OH bond. A new band appeared at 1139 cm^{-1}, and the O–FeOH bond was detected by an intense band at 1094 cm^{-1}. It can be assumed that a ferric complex had formed in the feed water. In other side, IR results were followed by UV spectrum analysis (Fig. S5 Supplementary content) which shows that the band of the ferric citrate(III) appeared in feed and in the rejected water, but it was absent in the permeate. Above observations lead to confirm that the addition of citric acid leads to an iron citrate complex formation in pretreatment; that specie was captured by the RO membrane and can be used as a remover for iron.

Recovery rate and pressure losses measurements

Previous results shown above confirm that the citric acid is able to complex ferrous ions and to build the Fe–Cit complex, which can be captured by RO membrane. However, the current paragraph addresses the effect of this complex on RO membranes performances such as recovery rate and pressure drop. Experimental measurements were monitored as a function of time and are presented in Fig S6 (supplementary content). Results showed that recovery
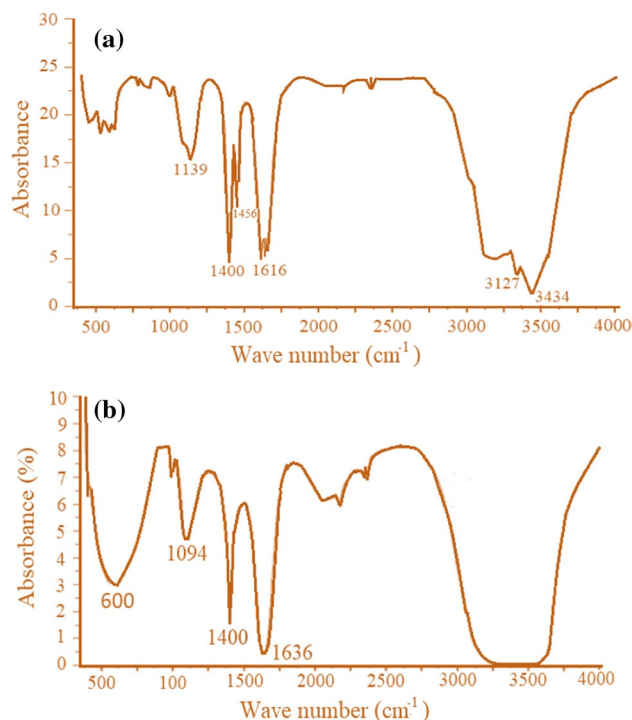
Fig. 7 IR spectra of **a** citric acid Cit^{3-}, **b** ferric citrate(III) complex formed in the feed water

ratio is approximately constant. However, during the fouling process, it decreased greatly. Therefore, it is logical to suggest that iron scaling phenomena did not occur with citric acid addition. The pressure drop kept its initial value of 1.5 bars. To evaluate the effect of the citric acid on the fouling process, iron accumulation rate was also used in this case. It was calculated as follows:

$$\tau = \frac{[Fe]_0 - [Fe]_P}{[Fe]_0} \tag{4}$$

where $[Fe]_0$ is the iron initial concentration and $[Fe]_p$ is the permeate iron concentration. Without citric acid addition, the iron accumulation rate (Fig. S7 supplementary content) rose up to 60%. However, with citric acid addition, iron accumulation rate rose up under 10%. These measurements showed strongly that iron oxides scale depends on citric acid addition. Moreover, Fig. 5S shows that the rejected water contains almost the totality of the Cit–Fe complex that previously existed on the feed water, which means that the

iron complex was removed by the membrane without being sticking in its surface. Therefore, it can be clearly seen that complexation–filtration technique is considerably efficient for iron removal. It can be used to avoid membrane fouling as well as cleaning process. In addition, the examination of membrane did not reveal any significant damage in terms of structure and performance. Meanwhile, the short time of operation does not allow confirming with high certitude that the addition of the cleaning reagent does not affect the membrane during excessive use.

Conclusion

Membrane fouling by iron oxides was studied herein. It was found that the performance of the RO membrane decreases significantly due to the precipitation of iron, despite the low initial concentration of ferrous ions. Qualitative studies were carried out to reveal the nature of the deposits. It was found that the goethite form precipitated on the surface of RO membrane, while the lepidocrocite form precipitated at the filter in the pretreatment step. During backwashing cleaning process, citric acid (0.01%) was proposed as a cleaning reagent. It was found that the fouled RO membrane regains its performance and recovery ratio of the process increased significantly. The citric acid was also tested for iron fouling inhibition due to its ability to complex the iron in aqueous solution. In fact, it reacts with iron to form the Fe–Cit complex. A concentration of 0.01% of citric acid was added to the feed water tank. Results showed no precipitation occurred on the surface of the membrane, and the Fe–Cit complex was found on the retentate of the RO process.

Compliance with ethical standards

Conflict of interest The authors declare that they have no conflict of interest.

References

Al-Anber MA (2010) Removal of high-level Fe^{3+} from aqueous solution using natural inorganic materials: bentonite (NB) and quartz (NQ). Desalination 250:885–891

Aziz HA, Yusoff MS, Adlan MN, Adnan NH, Alias S (2004) Physicochemical removal of iron from semi-aerobic landfill leachate by limestone filter. Waste Manag 724:353–358

Bobtesky M, Jordan J (1947) the structure and behavior of ferric tartrate and citrate complexes in dilute solutions. J Am Chem Soc 69:2286

Chivot J (1998) Selection of thermodynamic data concerning the Fe–H_2O system. Technical Report SCECF, 481

Chivot J (1999) Re-E-pH diagrams of the Fe–H_2O system as a function of temperature. Technical Report, 496

Cornel RM, Schwertmann U (1996) The iron oxides structure properties, reactions, occurrences and uses. VCH, Weinheim

Das B, Hazarika P, Saikia G, Kalita H, Goswami DC, Das HB, Dube SN, Dutta RK (2007) Removal of iron by groundwater by ash: a systematic study of a traditional method. Hazard Mater 141:834–841

Descostes M (2001) Evaluation of an oxidative perturbation in a clayey medium: mechanism of oxidation of pyrite. Ph.D. Thesis, Paris VII University, France

Ellis D, Bouchard C, Lantagne G (2000) Removal of iron and manganese from groundwater by oxidation and microfiltration. Desalination 130:255–264

Field TB, Mccourt JL, Mcbryde WAE (1974) Composition and stability of iron and copper citrate complexes in aqueous solution. Can J Chem 53:3119

Hamm RE, Schull CM, Grant DV (1954) Citrate complexes with iron(II) and iron(III). J Am Chem Soc 76:2111

Hidalgo AM, León G, Gómez M, Murcia MD, Gómez JL (2011) Modeling of aniline removal by reverse osmosis using different membranes. Chem Eng Technol 34:1753–1759

Ji J, Li J, Qiu J, Li X (2016) Polyacrylamide–starch composite flocculant as a membrane fouling reducer: key factors of fouling reduction. Sep Purif Technol 167:154–162

Kedem O, Katchalsky A (1958) Thermodynamic analysis of the permeability of biological membrane to non-electrolytes. Biochim Biophys Acta 27:229–249

Lanford OE, Quinan JR (1948) A spectrophotometric study of the reaction of ferric iron and citric acid. J Am Chem Soc 70:1948

Manning PG, Ramamoorthy S (1973) Equilibrium studies of metal-ion complexes of interest to natural waters: mixed ligand complexes of Cu(II) involving fulvic acid as primary ligand. Inorg Nucl Chem 35:1577–1581

Owusu-Agyeman I, Jeihanipour A, Luxbacher T, Schäfer AI (2007) Implications of humic acid, inorganic carbon and speciation on fluoride retention mechanisms in nanofiltration and reverse osmosis. Membr Sci 528:82–94

Peters T (2010) Membrane technology for water treatment. Chem Eng Technol 33:1233–1240

Refait P, Genin JMR (1997) the mechanisms of oxidation of ferrous hydroxychloride β-$Fe_2(OH)_3Cl$ in aqueous solution: the formation of akaganeite vs goethite. Corros Sci 39:539–553

Shapiro J (1964) Effect of yellow organic acids on iron and other metals in water. Am Water Works Assoc 56:1062–1082

Sung W, Morgan JJ (1980) Kinetics and product of ferrous iron oxygenation in aqueous systems. Environ Sci Technol 14:561–568

Tahir SS, Rauf N (2004) Removal of Fe^{2+} rom the waste water of a galvanized pipe manufacturing industry by adsorption onto bentonite clay. Environ Manag 73:285–292

Tipping E (1992) Cation binding by humic substance. Biochim Biophys Acta 56:3627–3641

Touati K, Tadeo F, Elfil H (2017a) Osmotic energy recovery from reverse osmosis using two-stage pressure retarded osmosis. Energy 132:213–224

Touati K, Jacobo S, Tadeo F, Elfil H (2017b) Energy recovery from two-stage SWRO plant using PRO without external freshwater feed stream: theoretical analysis. Renew Energy 105:84–95

Touati K, Hila M, Makhlouf K, Elfil H (2017c) Study of fouling in two-stage reverse osmosis desalination unit operating without an inlet pH adjustment: diagnosis and implications. Water Sci Technol Water Supply 18(3):1682–1693

Touati K, Cherif H, Kammoun N, Jendoubi M, Elfil H (2018a) Inhibition of calcium carbonate scaling by precipitation using secondary nucleation coupled to degassing with atmospheric air. J Water Process Eng 22:258–264

Touati K, Elbez A, Zendah H, Elfil H, Hannachi A (2018b) Sand filters scaling by calcium carbonate precipitation during groundwater reverse osmosis desalination. Desalination 430:24–32